Element scavenging by recently formed travertine deposits in the alkaline springs from the Oman Semail Ophiolite

Olsson, Jonas; Stipp, Susan Louise Svane; Gislason, S.R.

Published in:
Mineralogical Magazine

DOI:
10.1180/minmag.2014.078.6.15

Publication date:
2014

Document version
Publisher's PDF, also known as Version of record

Mineralogical Magazine, November 2014, Vol. 78(6), pp. 1479–1490

OPEN ACCESS

Element scavenging by recently formed travertine deposits in the alkaline springs from the Oman Semail Ophiolite

J. Olsson[1,2,*], S. L. S. Stipp[1] and S. R. Gislason[2]

[1] Nano-Science Center, Department of Chemistry, University of Copenhagen, Universitetsparken 5, DK-2100 København Ø, Denmark

[2] Nordic Volcanological Institute, Institute of Earth Sciences, University of Iceland, Sturlugata 7, 101 Reykjavik, Iceland

[*Received 6 May 2014; Accepted 9 December 2014; Associate Editor: T. Rinder*]

ABSTRACT

Ultramafic rocks, such as the Semail Ophiolite in the Sultanate of Oman, are considered to be a potential storage site for CO_2. This type of rock is rich in divalent cations that can react with dissolved CO_2 and form carbonate minerals, which remain stable over geological periods of time. Dissolution of the ophiolite mobilizes heavy metals, which can threaten the safety of surface and groundwater supplies but secondary phases, such as iron oxides, clays and carbonate minerals, can take up significant quantities of trace elements both in their structure and adsorbed on their surfaces.

Hyperalkaline spring waters issuing from the Semail Ophiolites can have pH as high as 12. This water absorbs CO_2 from air, forming carbonate mineral precipitates either as thin crusts on the surface of placid water pools or bottom precipitates in turbulent waters. We investigated the composition of the spring water and the precipitates to determine the extent of trace element uptake. We collected water and travertine samples from two alkaline springs of the Semail Ophiolite. Twenty seven elements were detected in the spring waters. The bulk of the precipitate was $CaCO_3$ in aragonite, as needles, and rhombohedral calcite crystals. Traces of dypingite ($Mg_5(CO_3)_4(OH)_2{\cdot}5H_2O$) and antigorite ($(Mg,Fe)_3Si_2O_5(OH)_4$) were also detected. The bulk precipitate contained rare earth elements and toxic metals, such as As, Ba, Cd, Sr and Pb, which indicated scavenging by the carbonate minerals. Boron and mercury were detected in the spring water but not in the carbonate phases. The results provide confidence that many of the toxic metals released by ophiolite dissolution in an engineered CO_2 injection project would be taken up by secondary phases, minimizing risk to water quality.

Keywords: travertine, ophiolite, CO_2 storage site, heavy metals.

Introduction

Capturing and storing CO_2 in rock as carbonate minerals, formed during injection of CO_2 into geological formations, has great potential for reducing atmospheric concentrations of anthropogenic CO_2. Some carbonate minerals form readily in nature but by increasing our understanding, the processes could be enhanced and used on an industrial scale. Improved understanding of carbonate mineral formation would also contribute towards more robust models for predicting the global carbon balance (Mackenzie and Andersson, 2013). Field-scale projects, where CO_2-charged waters are injected into the subsurface, have already begun, e.g. into basaltic formations in Iceland and northwestern USA (Alfredsson *et al*., 2008; Oelkers *et al*., 2008;

* E-mail: jolsson@nano.ku.dk
DOI: 10.1180/minmag.2014.078.6.15

This paper is published as part of a special issue in *Mineralogical Magazine*, Vol. **78(6)**, 2014 entitled 'Mineral–fluid interactions: scaling, surface reactivity and natural systems'.

Gislason *et al*., 2010; McGrail *et al*., 2011; Alfredsson *et al*., 2013; Gislason and Oelkers, 2014). Carbon dioxide-enriched waters are corrosive (at 1 atm CO_2, pH = 3.6) and when injected into geological formations, they attack the host rock, increasing weathering rates. Mafic and ultramafic rock releases ions such as Ca, Mg and Fe, which can combine with the dissolved CO_2 and form stable carbonate phases. The overall reaction is energetically favourable (Lackner *et al*., 1995) but depends on fluid composition, ionic strength, reduction potential, pH, temperature and total pressure (Stumm, 1992; Krauskopf and Bird, 1994; Gislason *et al*., 2010; Olsson *et al*., 2012). Mafic and ultramafic rocks are well suited to CO_2 storage because of their large divalent cation:Si ratio, and thus greater capacity for carbon capture, and lower tendency to form clay minerals, which use up cations, thus decreasing carbonation potential. Reaction in these rock formations neutralizes the acidic waters, thus promoting carbonate mineral precipitation. However, injecting CO_2-charged waters, and the ensuing dissolution of the host rock, can mobilize toxic heavy metals, such as As, Ba, Cd, Cr, F, Hg and Pb (Turekian and Wedepohl, 1961), which could pose a risk for surface and groundwater supplies (Aiuppa *et al*., 2000; Flaathen *et al*., 2009; Galeczka *et al*., 2013; Olsson *et al*., 2013; Galeczka *et al*., 2014; Olsson *et al*., 2014).

The Semail Ophiolite of the Sultanate of Oman is a potential site for CO_2-charged water injection for carbon sequestration (Kelemen and Matter, 2008; Matter and Kelemen, 2009; Paukert *et al*., 2012). It is one of the largest and best preserved ophiolites in the world and covers ~30,000 km^2, with an average thickness of ~5 km (Neal and Stanger, 1984*b*; Nicolas *et al*., 2000; Chavagnac *et al*., 2013*a*). About 30% of this volume is the ultramafic rock, peridotite, which contains mostly olivine and pyroxene and <45% silica (Nicolas *et al*., 2000; Kelemen and Matter, 2008). Groundwater dissolves the peridotite by reactions such as:

$$\underset{\text{Olivine}}{(Fe,Mg)_2SiO_4} + \underset{\text{Pyroxene}}{(Ca,Fe,Mg)SiO_3} + 6H^+ + H_2O \rightarrow 3(Ca^{2+},Fe^{2+},Mg^{2+}) + 2H_4SiO_4 \quad (1)$$

releasing cations and increasing pH. At low partial CO_2 pressure, intermediate products associated with the incomplete dissolution of peridotite are typically serpentine $(Mg,Fe)_3Si_2O_5(OH)_4$ and talc $(Mg_3Si_4O_{10}(OH)_2)$. Spring waters discharging from ultramafic rocks are extremely alkaline, with a pH as high as 12 and CO_2 partial pressure $<10^{-8}$ bars (Barnes *et al*., 1978; Neal and Stanger, 1984*a*; Paukert *et al*., 2012; Chavagnac *et al*., 2013*b*). As the hyperalkaline water emerges at the Earth's surface, it equilibrates with atmospheric CO_2, carbonate minerals become supersaturated at the air–water interface and precipitate (Fig. 1) by the overall reaction:

$$(Ca,Fe,Mg)^{2+} + CO_2 + H_2O \rightleftharpoons (Ca,Fe,Mg)CO_3 + 2H^+ \quad (2)$$

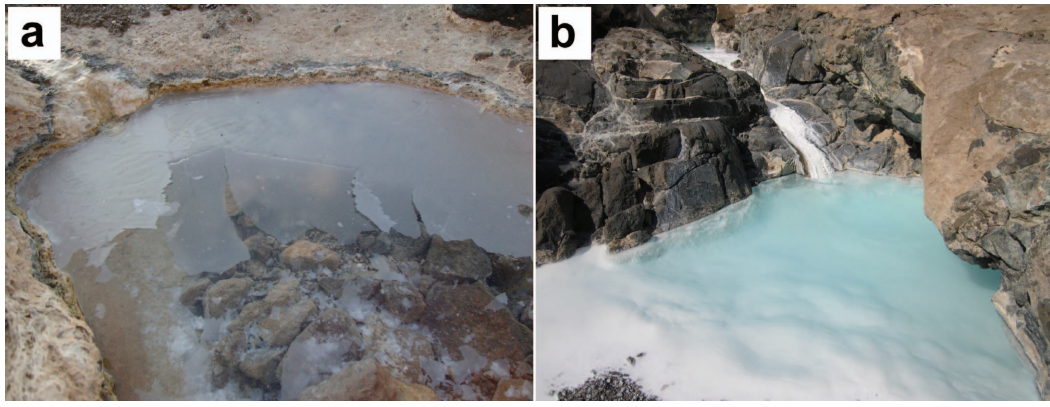

FIG. 1. Precipitation of carbonate minerals at the locations where Sample OM01 (*a*) and Sample OM08 (*b*) were collected. In calm hyperalkaline waters, the precipitation rate is controlled by the diffusion of CO_2 from the atmosphere through the air–water interface. Carbonate minerals form as a thin crust that looks like ice (*a*). In fast-moving spring waters (white waters), where the air–water surface film is broken, the nucleation and precipitation is homogenous within the water body (*b*).

As protons are released, pH decreases. The minerals observed are calcite and aragonite (both $CaCO_3$), as well as brucite ($Mg(OH)_2$) and antigorite ($(Mg,Fe)_3Si_2O_5(OH)_4$) (Neal and Stanger, 1984*a*; Chavagnac *et al*., 2013*a*). Spring waters in natural systems can be considered as an analogue for CO_2 injection into ophiolites in general (Kelemen and Matter, 2008; Beinlich *et al*., 2010, 2012; Paukert *et al*., 2012) and by studying the uptake of trace metals into the secondary phases, we can gain information about their mobility as a result of CO_2 injection. The aim of this study was to analyse ultramafic spring waters and the natural precipitated products to investigate the extent of trace element uptake into the solids and loss from the solution phase.

Sampling and analyses

The samples were collected on 13 and 14 January 2011, a total of eight liquid and eight solid samples from two alkaline springs in Oman. The springs were located near the village of Falaji (Spring #1) and Qafifah (Spring #2) discharging from partly serpentinized peridotite and gabbroic rocks. Samples from the two springs and the surroundings have been described elsewhere (Nicolas *et al*., 2000; Kelemen and Matter, 2008; Matter and Kelemen, 2009; Paukert *et al*., 2012; Chavagnac *et al*., 2013*a*,*b*). pH and alkalinity were measured in the field. The pH was measured using a plastic body, double junction electrode, connected to a CyberScan 310 pH meter, calibrated against certified buffers (pH 4.01, 7.00, 10.01 and 12.46) from Oakton. Electrode and buffers were at the same temperature as the spring water. Alkalinity was determined by Gran titration, using HCl (Gran, 1952; Stumm and Morgan, 1981). Samples for ion chromatography (IC) and inductively coupled plasma optical emission spectrometry (ICP-OES) were filtered in the field through 0.2 μm cellulose acetate membranes. They were collected in plastic vials that had been flushed three times with the sample. Samples for ICP-OES were acidified with concentrated, suprapure HNO_3 (1:100) onsite to prevent precipitation of solids during transport. An overview of the fluid samples and locations is found in Table 1.

Solid samples were collected in plastic bags and freeze dried for 24 h in the laboratory to minimize alteration. The solids were characterized by means of standard X-ray powder diffraction (XRD) and scanning electron microscopy (SEM), using instrument conditions and procedures described by Olsson *et al*. (2014). Residual water in the pores could not be removed by freeze drying and is responsible for precipitation of halite (NaCl) observed in the XRD patterns. The solid samples were flash dissolved in a 1% HNO_3 solution which dissolves the carbonate mineral phases while minimizing the dissolution of possible silicate mineral grains

TABLE 1. Summary of the sample data. At each location, a sample of travertine and spring water were collected. Samples OM01–05 were collected on 13 January 2011 in Spring #1 and Samples OM06, 07 and 08 were collected on 14 January 2011 in Spring #2.

Sample set	Distance from spring (m)	— Location — Latitude	Longitude	Water temperature (ºC)	pH	Total alkalinity (meq/l)
Spring #1						
OM01	0	22.8378	58.0568	30.6	11.6	5.9
OM02	5 ± 3	22.8379	58.0568	29.6	11.6	5.9
OM03	10 ± 3	22.8379	58.0567	26.8	11.7	6.3*
OM04	13 ± 3	22.8379	58.0567	25.3	11.6	5.8
OM05	18 ± 3	22.8380	58.0567	24.0	11.6	5.9
Spring #2						
OM06	0	22.9045	58.4245	20.3	11.5	3.2
OM07	15 ± 3	22.9044	58.4246	22.3	10.8	2.2
OM08	30 ± 3	22.9042	58.4249	20.3	10.9	1.9

* No filtration

originating from the ophiolite. Selected spring water and flash-dissolved samples were analysed at Analytica-SGAB, Luleå, Sweden, using ICP-OES and inductively coupled plasma sector field mass spectroscopy (ICP-SFMS). Mercury was measured with atomic fluorescence spectroscopy (AFS). The elements measured by IC were Cl^-, F^- and SO_4^{2-} and by ICP-OES were Al, As, B, Ba, Br, Ca, Cl, Cr, Fe, K, Li, Na, Mg, Mn, Mo, P, S, Sb, Si, Sr, Ti, V and W. In-house, multi-element standards were used for calibration and these are regularly tested against the Standard Canadian River Waters (SLRS-4) and single element international standards (SPEX). The uncertainties of the IC and ICP-OES data were estimated from analytical measurements. The reproducibility of duplicate samples for both methods is within 5%.

The geochemical speciation program *PHREEQC* (Parkhurst and Appelo, 1999), with the *MINTEQ* database (Allison *et al*., 1991), was used to determine the charge balance of the spring water samples, to estimate the dissolved inorganic carbon (DIC) and the saturation state of selected solid phases. The saturation state of lansfordite ($MgCO_3{\cdot}5H_2O$) was determined in a parallel *PHREEQC* operation run using the LLNL database (Wolery, 1992). The charge balance of all of the spring water samples was within 2% and ionic strength was <20 mM.

Results and interpretation

Spring-water chemistry

Five water samples were collected from Spring #1 and its runoff and three from Spring #2 and its runoff, at a series of sites downstream from the springs. At Spring #1, the pH was 11.6 and total alkalinity was 5.9 meq/l and these values remained constant downstream (Table 1). A summary of the dissolved components can be found in Tables 2 and 3. With the exception of the DIC, Mg, Ni and Zn, concentrations remained constant with distance downstream for Spring #1 (Fig. 2). The DIC increased as expected because of the influx of CO_2 from the atmosphere. Mg concentration was very low, ~6.3 μM, probably because it was controlled by the formation of serpentine, brucite or hydrotalcite (Neal and Stanger, 1984*b*; Paukert *et al*., 2012; Chavagnac *et al*., 2013*b*). The water in the pool near this spring was covered by a thin crust of solid $CaCO_3$, which inhibited influx of atmospheric CO_2. The constant composition of the spring water suggests that relatively little of the dissolved elements formed precipitates. The reasons are: (1) the short period during which precipitates could form during the time the water emerged from the spring outlet to 20 to 30 m downstream, where the last sample was collected; and (2) carbonate minerals could not precipitate because the concentration of dissolved carbonate was hindered by the thin crust of $CaCO_3$ at the water surface (Fig. 1*a*). The influx of CO_2 depends on water turbulence, i.e. dissolution is faster when the gas forms foam and bubbles during mixing, such as at waterfalls, breaking waves or rapid transport (Jähne *et al*., 1987; Gislason *et al*., 1996). The water of Spring #1 experienced only slight turbulence, therefore slow CO_2 influx.

At Spring #2, pH decreased significantly from 11.5 to 10.9 downstream and alkalinity, from 3.2 to 1.9 meq/l (Table 1). Ca, K, Mg, Si, SO_4 and Sr decreased slightly downstream; Ba, Br, Cl and Na increased slightly. In the last sample, F increased by a factor 5 (Fig. 3). The complicated changes in the chemical composition suggest multiple dissolution/precipitation reactions and possible input from a second spring. The DIC increased from 0.22 mM to 0.83 mM over the first 15 m but decreased again to 0.65 mM at 30 m. Precipitation of carbonate minerals consumes DIC. It is likely that magnesium carbonates formed because the Mg concentration in Spring #2 decreased with distance downstream and was more than 2 orders higher than the Mg concentration in Spring #1. Spring #2 water fell over a series of short drops so the turbulence increased the CO_2 influx much more than at the calm water−air interface at site OM01 (Fig. 1). CO_2 uptake decreased the pH. Rapid influx promoted fast carbonate mineral precipitation, where the rate was limited by nucleation and growth within the water body rather than by CO_2 absorption only. Alternatively, the presence of a second spring could discharge water with lower pH and higher DIC into the stream bed, which would promote precipitation.

The water from both Springs #1 and #2 contains several elements which, at high concentration, pose a threat to water quality (Table 2). However, the concentrations of all of these elements are under the WHO threshold limits for clean drinking water (WHO, 2008). Many of the potentially toxic elements in these waters are likely to be scavenged by the precipitating travertine phases (Olsson *et al*., 2014).

TABLE 2. The element concentration of the solid travertine and the spring waters from the two sites. The travertine concentrations were normalized to one mole of $CaCO_3$. Concentration of the elements in the travertine and spring water which potentially pose a threat to the quality of groundwater supplies are included and the WHO standard for drinking water is shown for comparison (WHO, 2008). All concentrations in the spring waters are below the recommend limits of WHO. The precipitating travertine scavenges all toxic elements except Hg.

Spring	As	B	Ba	Cd	Cr	Cu	F	Hg	Mn	Mo	Ni	Pb
Spring waters (unit: nM)												
#1	BDL	BDL	19.2	BDL	BDL	11	5.89×10^{-3}	0.232	3.68	BDL	7.99	0.196
#2	BDL	4700	0.442	BDL	0.819	BDL	1.91×10^{-3}	4.84×10^{-2}	0.881	10.1	9.46	8.06×10^{-2}
WHO threshold	1.3×10^{2}	4.6×10^{4}	5.1×10^{3}	27	9.6×10^{2}	3.1×10^{4}	7.9×10^{4}	30	7.3×10^{3}	7.3×10^{2}	1.2×10^{3}	48
Solid travertine (unit: mmol/mol of $CaCO_3$)												
#1	7.7×10^{-5}	BDL	8.78×10^{-3}	3.1×10^{-6}	2.1×10^{-4}	3.7×10^{-4}	NA	BDL	9.51×10^{-3}	BDL	2.61×10^{-3}	6.9×10^{-5}
#2	4.8×10^{-5}	BDL	4.14×10^{-2}	4.0×10^{-6}	2.1×10^{-4}	2.7×10^{-4}	NA	BDL	1.77×10^{-2}	8.6×10^{-6}	1.33×10^{-3}	9.6×10^{-6}

BDL, below detection limit. The detection limits are (mM): As, 4×10^{-6}; B, 9×10^{-4}; Cd, 2×10^{-8}; Cr, 2×10^{-7}; and Mo, 5×10^{-7}.

TABLE 3. The element concentration of the solid travertine and the spring waters from sites. The travertine concentrations were normalized to one mole of $CaCO_3$. Small amounts of other elements were detected in the travertine, including Ce, Dy, Er, Eu, Gd, Ho, La, Nd, Pr, Sm, Tb, Tm and Yb.

	Ca	Al	Co	Fe	K	Mg	Na	P	Si	Sr	Ti	V	Zn
Spring waters (unit: mM)													
#1	2.15	1.6×10^{-4}	1×10^{-7}	4.7×10^{-5}	0.255	1.72×10^{-3}	9.5	7.2×10^{-5}	0.00407	0.00115	5×10^{-7}	1.4×10^{-6}	4.8E-05
#2	0.0314	8.6×10^{-6}	3×10^{-7}	BDL	0.0814	1.52	3.8	BDL	0.163	1.4×10^{-5}	BDL	3.0×10^{-6}	BDL
Solid travertine (unit: mmol/mol of $CaCO_3$)													
#1	–	0.0354	2.5×10^{-4}	1.78×10^{-2}	0.286	0.964	26	0.0218	0.146	0.495	1.9×10^{-4}	1.7×10^{-4}	6.11×10^{-3}
#2	–	0.0157	2.6×10^{-4}	1.04×10^{-2}	BDL	11.3	5.8	0.0128	0.850	2.26	1.9×10^{-5}	2.8×10^{-5}	8.85×10^{-3}

BDL, below detection limit. The detection limits are (mM): Ce, 4×10^{-8}; Dy, 3×10^{-8}; Er, 3×10^{-8}; Eu, 3×10^{-8}; Fe, 7×10^{-6}; Gd, 3×10^{-8}; Ho, 3×10^{-8}; La, 4×10^{-8}; Lu, 3×10^{-8}; Nd, 3×10^{-8}; P, 2×10^{-5}; Pr, 4×10^{-8}; Sm, 3×10^{-8}; Tb, 3×10^{-8}; Th, 9×10^{-8}; Ti, 2×10^{-8}; Tm, 2×10^{-8}; and Yb, 3×10^{-8}.

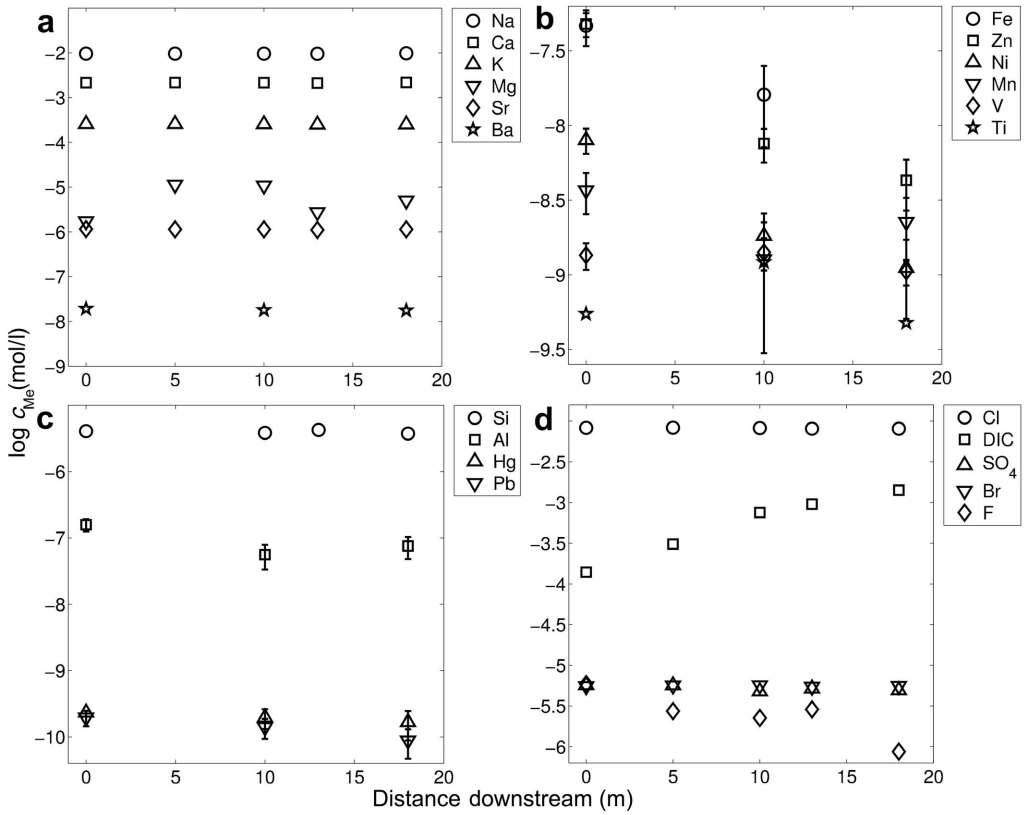

FIG. 2. Element concentrations in the stream water measured with distance downstream in Spring #1, including the concentration of (*a*) the alkali and alkali earth metals, (*b*) transition metals, (*c*) other metals of interest, and (*d*) anions. The dissolved inorganic carbon was estimated using *PHREEQC*. Most concentrations remain constant with distance downstream except for Mg, Fe, Ni and Zn. Uncertainty is generally within the dimension of the symbols. No uncertainty limits are available for Ti.

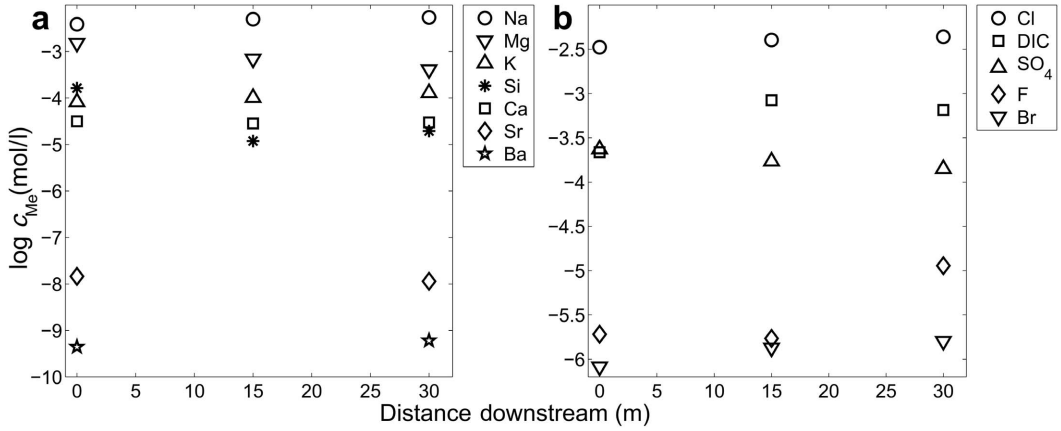

FIG. 3. Element concentrations measured as a function of distance downstream in Spring #2, including the concentration of (*a*) the alkali metals, alkali earth metals and Si, and (*b*) anions. The dissolved inorganic carbon was estimated using *PHREEQC*. Uncertainties are within the dimension of the symbols.

The travertine deposits

The travertine deposits in the alkaline springs were analysed using XRD and SEM/EDXS to identify the mineral composition and the morphology of the samples collected. The precipitates of the springs consist mainly of aragonite and calcite. The XRD patterns of the samples from Spring #1 also showed traces of dypingite ($Mg_5(CO_3)_4(OH)_2{\cdot}5H_2O$), antigorite ($(Mg,Fe)_3Si_2O_5(OH)_4$) and halite (NaCl). We were not able to detect amorphous material. With the exception of halite, these precipitates are typical of the hyperalkaline springs of the Oman ophiolites (Neal and Stanger, 1984*a*; Chavagnac *et al*., 2013*a*). The presence of halite can be explained by evaporation of residual water when the samples were freeze dried. The SEM images of the thin-surface precipitate show rhombohedral calcite in a network of aragonite crystals (Figs 1*a*, 4*a*), whereas the precipitate from the bottom of Spring #1 consisted of dypingite rosettes with bouquets of aragonite (Fig. 4*b*). The XRD patterns showed that the travertine samples from Spring #2 were predominantly of aragonite. The SEM images showed small networks of rosettes growing on aragonite needles (Fig. 4*c*,*d*). The rosettes were rich in magnesium, indicating either dypingite or brucite (Power *et al*., 2007; Chavagnac *et al*., 2013*a*).

The chemical composition of the carbonate minerals in the travertine samples was quantified by flash dissolving the samples and analysing the chemical components released to solution. The average composition for travertine from both springs was determined and normalized to one mole of dissolved $CaCO_3$, assuming all Ca ions originated from pure $CaCO_3$ (Table 2 and 3). The travertine contains a wide range of elements, including rare earth elements (*REE*) and the toxic elements: As, Ba, Cd, Cr, Cu, Mn, Mo, Ni and Pb. Some elements were below detection limits in the spring water but were found in the travertine which indicates that these trace elements have, to a significant extent, been taken up by the precipitates. Elements observed in the spring waters were also found in the travertine, except for B and Hg. Thus, most toxic elements released from an engineered CO_2 injection project would be sequestered by secondary minerals but some, namely B and Hg, would not.

Mineral saturation estimated using PHREEQC

Numerous carbonate minerals can form in the alkaline spring waters of Oman. We investigated which phases are supersaturated and evaluated if they would be likely to precipitate while the spring water equilibrated with atmospheric CO_2. Knowing which phases are present in the travertine is important because trace element coprecipitation and adsorption are controlled by the composition and structure of the sorbing phase. We used the *PHREEQC* geochemical speciation model to determine the saturation states. In the model, CO_2 was added to the spring water in small steps and the saturation states were calculated until equilibrium with atmospheric CO_2 was reached (SI = −3.4). No minerals were allowed to precipitate. For the model, we used data from Sample OM01 (water from Spring #1) and OM06 (from Spring #2), including temperature, chemical composition, pH and alkalinity. The saturation index (SI) maximum at pH 10.6, for the pure carbonate phases, corresponds to the point at which the CO_3^{2-} concentration peaks. At lower pH, the HCO_3^- ion dominates.

PHREEQC predicted that the supersaturated phases in Spring #1 would be calcite (hexagonal $CaCO_3$), aragonite (orthorhombic $CaCO_3$) and dolomite ($CaMg(CO_3)_2$) and in Spring #2, artinite ($Mg_2(CO_3)(OH)_2{\cdot}3H_2O$), dolomite, huntite ($Mg_3Ca(CO_3)_4$), magnesite ($MgCO_3$), hydromagnesite ($Mg_5(CO_3)_4(OH)_2{\cdot}4H_2O$), calcite and aragonite (Fig. 5). Lansfordite ($MgCO_3{\cdot}5H_2O$, not shown) and nesquehonite ($MgCO_3{\cdot}3H_2O$) were predicted to be undersaturated. Inorganic synthesis of dolomite, magnesite and huntite at atmospheric pressure and temperature below 40ºC has never been reported (Deelman, 1999; Saldi *et al*., 2009; Deelman, 2011; dos Anjos *et al*., 2011) so they are not expected to precipitate in the Oman spring waters. Hydrous magnesium carbonate phases, such as artinite, hydromagnesite and dypingite ($Mg_5(CO_3)_4(OH)_2{\cdot}5H_2O$), are far more likely to form (Hsu, 1967; Botha and Strydom, 2001; Hopkinson *et al*., 2008; Hänchen *et al*., 2008). No thermodynamic data are available for predicting the saturation state of dypingite but precipitation of both dypingite and hydromagnesite can be mediated by microorganisms (Ming and Franklin, 1985; Braithwaite and Zedef, 1996; Power *et al*., 2007; Cheng and Li, 2009; Power *et al*., 2009). The hydrous magnesium carbonate minerals are relatively stable and form more readily than magnesite at temperatures of <80ºC and they have therefore been suggested as alternative reaction products for carbonate storage (Ballirano *et al*., 2013). The magnesium concentration in the outlet spring waters is very

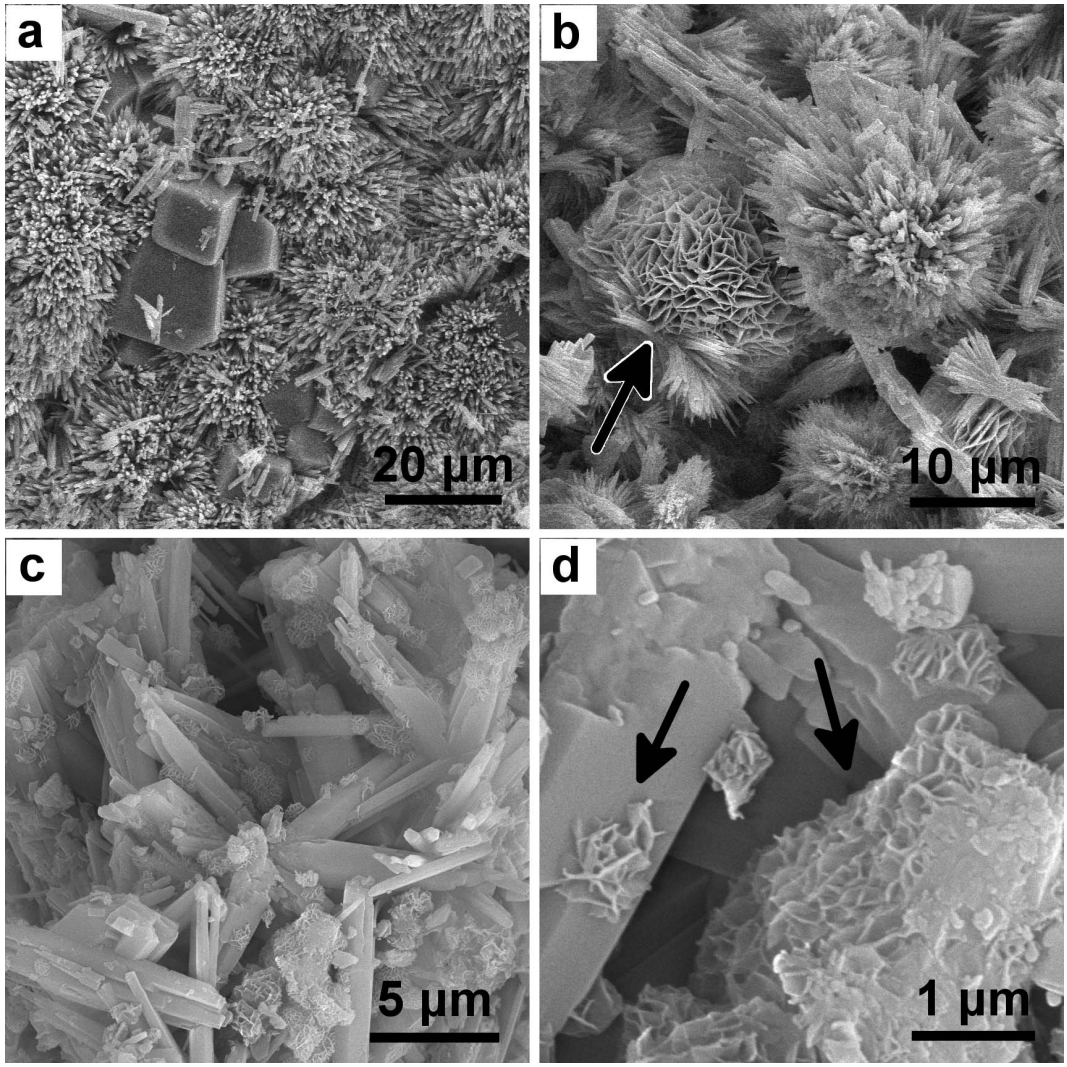

FIG. 4. SEM images of the precipitates from Spring #1 (*a*,*b*) and Spring #2 (*c*,*d*). (*a*) The carbonate surface film from Fig. 1*a*, sample OM01: rhombohedral calcite in a network of aragonite needles. (*b*) Sample OM03, dypingite rosettes (black arrow) surrounded by acicular aragonite; (*c*) Sample OM08 from Fig. 1*b*, crystals of aragonite; (*d*) close-up of the same area showing a secondary phase (black arrows) growing from or nucleating on the aragonite crystals. These crystals are probably dypingite. Samples OM03 and OM08 were collected from the bottom of the springs.

low as a result of serpentinization. In an engineered CO_2 injection scenario, serpentinization is expected to be minimal and therefore the relative concentration of Mg would be much higher, i.e. ~50 times higher than the Ca concentration (Boudier and Coleman, 1981). In this scenario, magnesium phases would probably dominate the secondary phases and these could complement the scavenging of contaminants above that observed in this study. More research is needed to confirm this assessment.

Conclusions and outlook

The spring waters from the Semail Ophiolite are highly alkaline, with pH between 11.6 and 10.9.

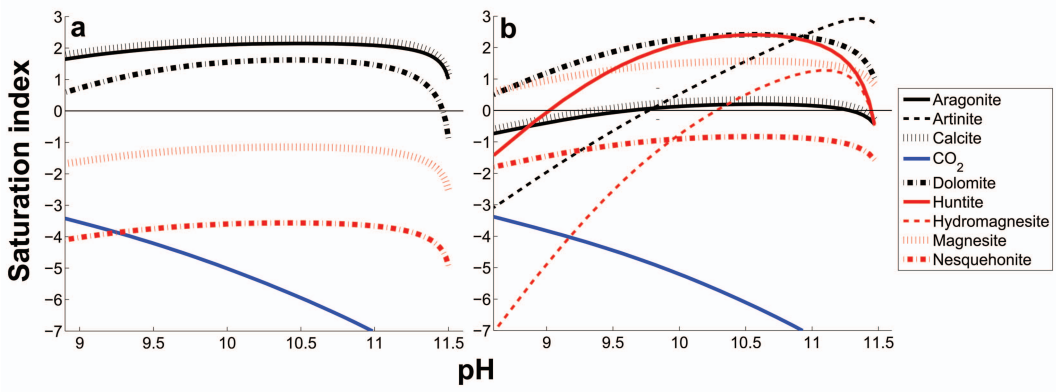

FIG. 5. The saturation state of selected carbonate minerals as a function of pH (addition of CO_2) with respect to the water from (*a*) Spring #1 at Sampling site OM01, and (*b*) Spring #2 at Sampling site OM06. Secondary minerals were not allowed to precipitate in the model. The reaction progress is from right to left in the figures. Before the addition of CO_2, the pH was 11.6 and temperature was 30.6ºC for Spring #1, and 11.5 and 20.3ºC for Spring #2. The logarithm of the initial partial pressure of CO_2 was −9.3 bar for Spring #1 water and −8.3 bar in Spring #2. The logarithm of the final CO_2 pressure after the solution reached equilibrium with the Earth's atmosphere was −3.4 bar or 395 ppm CO_2.

The most prominent cations are Ca, K, Na, Mg and Si; anions are Br, Cl, F and SO_4. Within uncertainty, the concentrations remain constant downstream for Spring #1 but complicated changes in the chemical composition for Spring #2 suggest dissolution and precipitation reactions and probably input from a second spring.

Travertine samples from the alkaline springs consist of aragonite often mixed with calcite and traces of dypingite and antigorite. Other phases that were supersaturated in the spring waters, and predicted to precipitate at atmospheric conditions, were artinite and hydromagnesite. The most common alkali, alkali earth and transition metals were detected in the solid travertine samples along with *REE* and toxic elements such as As, Ba, Cd, Cr, Cu, Mn, Mo, Ni and Pb. This suggests active and effective scavenging by precipitation of the carbonate minerals, thus limited mobility of contaminants. However, boron and mercury were not removed from the water. If they were present at increased concentrations they would pose a health risk.

Our study shows that several carbonate minerals precipitate readily in groundwater from the Semail Ophiolite when CO_2 dissolves in it. Aragonite and calcite dominate the precipitates and these phases are well known to incorporate trace elements. Thus we can conclude that toxic metals that are released during dissolution of the ophiolite are taken up by the travertine. From this we can draw analogies with likely scenarios for geological CO_2 sequestration. Although the reaction conditions in an engineered CO_2 injection system would be different from the conditions in our study, in both cases, Ca, Mg, Fe, CO_2 and trace metals would be present and where carbonate minerals such as calcite reach supersaturation and precipitate, we would expect the precipitates to scavenge the trace elements. Thus we can conclude that if toxic trace metals are released by dissolution of mafic or ultramafic rocks during CO_2 injection, they would probably be sequestered by the carbonate minerals or other secondary phases (such as Fe oxides and clays) that form as the waters approach equilibrium.

Thus, this ophiolite system serves as a natural analogue, providing insight into what could be expected from engineered injection of CO_2 into porous peridotite and offers an example scenario of what might happen if CO_2 leaks from an injection site. Such studies of natural analogues are useful for providing information about natural processes that laboratory studies of ideal systems cannot. Studying natural systems gives information about how elements or products are favoured or disfavoured in complicated competitive reactions.

Acknowledgements

The authors thank Eydís Salome Eiríksdóttir, Helene Almind and Iwona Gałeczka for technical help. For assistance in the field and transport of the samples, Pablo García del Real and Amelia

Paukert are acknowledged. The authors are also grateful to Christophe Monnin and two anonymous reviewers for their comments during review. The work was funded by the Nordic Volcanological Institute (NORDVULK), the Institute of Earth Sciences, Reykjavík, Iceland; the NanoGeoScience Group, Nano-Science Center, Department of Chemistry, Copenhagen, Denmark; a travel grant for the IODP/ICDP Workshop on "Geological carbon capture & storage in mafic and ultramafic rocks" sponsored by the ESF Magellan Workshop Series; and by the European Commission Framework 7, through the CarbFix Project, Grant Agreement No: FP7 283148.

References

Aiuppa, A., Allard, P., D'Alessandro, W., Michel, A., Parello, F., Treuil, M. and Valenza, M. (2000) Mobility and fluxes of major, minor and trace metals during basalt weathering and groundwater transport at Mt. Etna volcano (Sicily). *Geochimica et Cosmochimica Acta*, **64**, 1827–1841.

Alfredsson, H.A., Hardarson, B.S., Franzson, H. and Gislason, S.R. (2008) CO_2 sequestration in basaltic rock at the Hellisheidi site in SW Iceland: stratigraphy and chemical composition of the rocks at the injection site. *Mineralogical Magazine*, **72**, 1–5.

Alfredsson, H.A., Oelkers, E.H., Hardarsson, B.S., Franzson, H., Gunnlaugsson, E. and Gislason, S.R. (2013) The geology and water chemistry of the Hellisheidi, SW-Iceland carbon storage site. *International Journal of Greenhouse Gas Control*, **12**, 399–418.

Allison, J.D., Brown, D.S. and Novo-Gradac, K.J. (1991) *MINTEQA2/PRODEFA2, a geochemical assessment model for environmental systems: Version 3.0 User's Manual*. EPA/600/3-91/021, US Environmental Protection Agency, Athens, Georgia, USA.

Ballirano, P., De Vito, C., Mignardi, S. and Ferrini, V. (2013) Phase transitions in the Mg-CO_2-H_2O system and the thermal decomposition of dypingite, $Mg_5(CO_3)_4(OH)_2{\cdot}5H_2O$: implications for geosequestration of carbon dioxide. *Chemical Geology*, **340**, 59–67.

Barnes, I., Oneil, J.R. and Trescases, J.J. (1978) Present day serpentinization in New Caledonia, Oman and Yugoslavia. *Geochimica et Cosmochimica Acta*, **42**, 144–145.

Beinlich, A., Austrheim, H., Glodny, J., Erambert, M. and Andersen, T.B. (2010) CO_2 sequestration and extreme Mg depletion in serpentinized peridotite clasts from the Devonian Solund basin, SW Norway. *Geochimica et Cosmochimica Acta*, **74**, 6935–6964.

Beinlich, A., Plumper, O., Hovelmann, J., Austrheim, H. and Jamtveit, B. (2012) Massive serpentinite carbonation at Linnajavri, N Norway. *Terra Nova*, **24**, 446–455.

Botha, A. and Strydom, C.A. (2001) Preparation of a magnesium hydroxy carbonate from magnesium hydroxide. *Hydrometallurgy*, **62**, 175–183.

Boudier, F. and Coleman, R.G. (1981) Cross section through the peridotite in the Samail Ophiolite, southeastern Oman Mountains. *Journal of Geophysical Research: Solid Earth*, **86**, 2573–2592.

Braithwaite, C.J.R. and Zedef, V. (1996) Hydromagnesite stromatolites and sediments in an alkaline lake, Salda Golu, Turkey. *Journal of Sedimentary Research*, **66**, 991–1002.

Chavagnac, V., Ceuleneer, G., Monnin, C., Lansac, B., Hoareau, G. and Boulart, C. (2013*a*) Mineralogical assemblages forming at hyperalkaline warm springs hosted on ultramafic rocks: a case study of Oman and Ligurian ophiolites. *Geochemistry, Geophysics, Geosystems*, **14**, 1–22.

Chavagnac, V., Monnin, C., Ceuleneer, G., Boulart, C. and Hoareau, G. (2013*b*) Characterization of hyperalkaline fluids produced by low-temperature serpentinization of mantle peridotites in the Oman and Ligurian ophiolites. *Geochemistry, Geophysics, Geosystems*, **14**, 2496–2522.

Cheng, W. and Li, Z. (2009) Precipitation of nesquehonite from homogeneous supersaturated solutions. *Crystal Research Technology*, **44**, 937–947.

Deelman, J.C. (1999) Low-temperature nucleation of magnesite and dolomite. *Neues Jahrbuch für Mineralogie Monatshefte*, 289–302.

Deelman, J.C. (2011) *Low-temperature formation of dolomite and magnesite*. Compact Disc Publications, Eindhoven, The Netherlands.

dos Anjos, A.P.A., Sifeddine, A., Sanders, C.J. and Patchineelam, S.R. (2011) Synthesis of magnesite at low temperature. *Carbonates and Evaporites*, **26**, 213–215.

Flaathen, T.K., Gislason, S.R., Oelkers, E.H. and Sveinbjornsdottir, A.E. (2009) Chemical evolution of the Mt. Hekla, Iceland, groundwaters: a natural analogue for CO_2 sequestration in basaltic rocks. *Applied Geochemistry*, **24**, 463–474.

Galeczka, I., Wolff-Boenisch, D. and Gislason, S.R. (2013) Experimental studies of basalt-H_2O-CO_2 interaction with a high pressure column flow reactor: the mobility of metals. *Energy Procedia*, **37**, 5823–5833.

Galeczka, I., Wolff-Boenisch, D., Oelkers, E.H. and Gislason, S.R. (2014) An experimental study of basaltic glass-H_2O-CO_2 interaction at 22 and 50ºC:

implications for subsurface storage of CO_2. *Geochimica et Cosmochimica Acta*, **126**, 123–145.

Gislason, S.R. and Oelkers, E.H. (2014) Carbon storage in basalt. *Science*, **344**, 373–374.

Gislason, S.R., Arnorsson, S. and Armannsson, H. (1996) Chemical weathering of basalt in southwest Iceland: effects of runoff, age of rocks and vegetative/glacial cover. *American Journal of Science*, **296**, 837–907.

Gislason, S.R., Wolff-Boenisch, D., Stefansson, A., Oelkers, E.H., Gunnlaugsson, E., Sigurdardottir, H., Sigfusson, B., Broecker, W.S., Matter, J.M., Stute, M., Axelsson, G. and Fridriksson, T. (2010) Mineral sequestration of carbon dioxide in basalt: a pre-injection overview of the CarbFix project. *International Journal of Greenhouse Gas Control*, **4**, 537–545.

Gran, G. (1952) Determination of the equivalence point in potentiometric titrations. Part II. *Analyst*, **77**, 661–671.

Hopkinson, L., Rutt, K. and Cressey, G. (2008) The transformation of nesquehonite to hydromagnesite in the system CaO-MgO-H_2O-CO_2: an experimental FT-Raman spectroscopic study. *Journal of Geology*, **116**, 387–400.

Hsu, K.J. (1967) Chemistry of Dolomite Formation. Pp. 169–191 in: *Carbonate Rocks – Physical and Chemical Aspects* (G.V. Chilingar, H.J. Bissell, and R.W. Fairbridge, editors). Developments in Sedimentology, Elsevier, Amsterdam.

Hänchen, M., Prigiobbe, V., Baciocchi, R. and Mazzotti, M. (2008) Precipitation in the Mg-carbonate system – effects of temperature and CO_2 pressure. *Chemical Engineering Science*, **63**, 1012–1028.

Jähne, B., Münnich, K.O., Bösinger, R., Dutzi, A., Huber, W. and Libner, P. (1987) On the parameters influencing air-water gas exchange. *Journal of Geophysical Research C: Oceans*, **92**, 1937–1949.

Kelemen, P.B. and Matter, J. (2008) In situ carbonation of peridotite for CO_2 storage. *Proceedings of the National Academy of Science, USA*, **105**, 17295–17300.

Krauskopf, K.B. and Bird, D.K. (1994) *Introduction to Geochemistry*. McGraw-Hill College, New York.

Lackner, K.S., Wendt, C.H., Butt, D.P., Joyce, E.L. and Sharp, D.H. (1995) Carbon dioxide disposal in carbonate minerals. *Energy*, **20**, 1153–1170.

Mackenzie, F.T. and Andersson, A.J. (2013) The marine carbon system and ocean acidification during Phanerozoic time. *Geochemical Perspectives*, **2**, 1–227.

Matter, J.M. and Kelemen, P.B. (2009) Permanent storage of carbon dioxide in geological reservoirs by mineral carbonation. *Nature Geoscience*, **2**, 837–841.

McGrail, B.P., Spane, F.A., Sullivan, E.C., Bacon, D.H. and Hund, G. (2011) The Wallula basalt sequestration pilot project. *Energy Procedia*, **4**, 5653–5660.

Ming, D.W. and Franklin, W.T. (1985) Synthesis and characterization of lansfordite and nesquehonite. *Soil Science Society of America Journal*, **49**, 1303–1308.

Neal, C. and Stanger, G. (1984*a*) Calcium and magnesium-hydroxide precipitation from alkaline groundwaters in Oman, and their significance to the process of serpentinization. *Mineralogical Magazine*, **48**, 237–241.

Neal, C. and Stanger, G. (1984*b*) Past and present serpentinisation of ultramafic rocks; an example from the Semail ophiolite nappe of Northern Oman. Pp. 249–275 in: *The Chemistry of Weathering* (J.I. Drever, editor). D. Reidel, Dordrecht, The Netherlands.

Nicolas, A., Boudier, E., Ildefonse, B. and Ball, E. (2000) Accretion of Oman and United Arab Emirates ophiolite – discussion of a new structural map. *Marine Geophysical Research*, **21**, 147–179.

Oelkers, E.H., Gislason, S.R. and Matter, J. (2008) Mineral carbonation of CO_2. *Elements*, **4**, 333–337.

Olsson, J., Bovet, N., Makovicky, E., Bechgaard, K., Balogh, Z. and Stipp, S.L.S. (2012) Olivine reactivity with CO_2 and H_2O on a microscale: implications for carbon sequestration. *Geochimica et Cosmochimica Acta*, **77**, 86–97.

Olsson, J., Stipp, S.L.S., Dalby, K.N. and Gislason, S.R. (2013) Rapid release of metal salts and nutrients from the 2011 Grímsvötn, Iceland volcanic ash. *Geochimica et Cosmochimica Acta*, **123**, 134–149.

Olsson, J., Stipp, S.L.S., Makovicky, E. and Gislason, S.R. (2014) Metal scavenging by calcium carbonate at the Eyjafjallajökull volcano: a carbon capture and storage analogue. *Chemical Geology*, **384**, 135–148.

Paukert, A.N., Matter, J.M., Kelemen, P.B., Shock, E.L. and Havig, J.R. (2012) Reaction path modeling of enhanced in situ CO_2 mineralization for carbon sequestration in the peridotite of the Samail Ophiolite, Sultanate of Oman. *Chemical Geology*, **330–331**, 86–100.

Power, I.M., Wilson, S.A., Thom, J.M., Dipple, G.M. and Southam, G. (2007) Biologically induced mineralization of dypingite by cyanobacteria from an alkaline wetland near Atlin, British Columbia, Canada. *Geochemical Transactions*, **8**, 13–13.

Power, I.M., Wilson, S.A., Thom, J.M., Dipple, G.M., Gabites, J.E. and Southam, G. (2009) The hydromagnesite playas of Atlin, British Columbia, Canada: a biogeochemical model for CO_2 sequestration. *Chemical Geology*, **260**, 286–300.

Saldi, G.D., Jordan, G., Schott, J. and Oelkers, E.H. (2009) Magnesite growth rates as a function of temperature and saturation state. *Geochimica et Cosmochimica Acta*, **73**, 5646–5657.

Stumm, W. (1992) *Chemistry of the Solid–Water*

Interface: Processes at the Mineral–Water and Particle–Water Interface in Natural Systems. Wiley, New York.

Stumm, W. and Morgan, J. J. (1981) *Aquatic Chemistry: an Introduction emphasizing Chemical Equilibria in Natural Waters*. Wiley, New York.

Turekian, K.K. and Wedepohl, K.H. (1961) Distribution of the elements in some major units of the earth's crust. *Geological Society of America Bulletin*, **72**, 175–192.

WHO (2008) *Guidelines for Drinking-Water Quality*. World Health Organization, Geneva.

Wolery, T.J. (1992) *EQ3/6, A Software Package for Geochemical Modeling of Aqueous Systems*. Lawrence Livermore National Laboratory Report, California, USA, UCRL-MA-110662 PT I.